



**HAL**  
open science

## Short remarks about synthetic image generation in the context of sub-pixel accuracy of Digital Image Correlation

Michel Bornert, Pascal Doumalin, Jean-Christophe Dupré, Christophe Poilâne, Laurent Robert, Evelyne Toussaint, Bertrand Wattrisse

### ► To cite this version:

Michel Bornert, Pascal Doumalin, Jean-Christophe Dupré, Christophe Poilâne, Laurent Robert, et al.. Short remarks about synthetic image generation in the context of sub-pixel accuracy of Digital Image Correlation. ICEM15 - 15th International Conference on Experimental Mechanics, Jul 2012, Porto, Portugal. 9 p. hal-00836213

**HAL Id: hal-00836213**

<https://hal.science/hal-00836213v1>

Submitted on 22 Nov 2021

**HAL** is a multi-disciplinary open access archive for the deposit and dissemination of scientific research documents, whether they are published or not. The documents may come from teaching and research institutions in France or abroad, or from public or private research centers.

L'archive ouverte pluridisciplinaire **HAL**, est destinée au dépôt et à la diffusion de documents scientifiques de niveau recherche, publiés ou non, émanant des établissements d'enseignement et de recherche français ou étrangers, des laboratoires publics ou privés.



Distributed under a Creative Commons Attribution - NonCommercial 4.0 International License

# SHORT REMARKS ABOUT SYNTHETIC IMAGE GENERATION IN THE CONTEXT OF THE ASSESSMENT OF SUB-PIXEL ACCURACY OF DIGITAL IMAGE CORRELATION

M. Bornert<sup>1</sup>, P. Doumalin<sup>2</sup>, J.C. Dupré<sup>2</sup>, C. Poilâne<sup>3,4</sup>, L. Robert<sup>5(\*)</sup>, E. Toussaint<sup>6</sup>, B. Wattrisse<sup>7</sup>  
On behalf of the Workgroup “Metrology” of the French CNRS research network 2519 “Mesures de Champs et Identification en Mécanique des Solides / Full-field measurements and identification in solid mechanics”.  
URL: [http:// www.gdr2519.cnrs.fr](http://www.gdr2519.cnrs.fr)

<sup>1</sup>Laboratoire Navier, École des Ponts ParisTech, Université Paris-Est, Marne-la-Vallée, France

<sup>2</sup>Institut P<sup>2</sup>, UPR 3346 CNRS, Université de Poitiers, SP2MI, Futuroscope Chasseneuil, France

<sup>3</sup>CIMAP, UMR6252, Université de Caen Basse-Normandie, CNRS, CEA, ENSICAEN, Caen, France

<sup>4</sup>LAUM, UMR 6613, CNRS, Université du Maine, Le Mans, France

<sup>5</sup>Institut Clément Ader ; Université de Toulouse ; Mines Albi, INSA, UPS, ISAE ; Albi, France

<sup>6</sup>Institut Pascal, UMR6602, Université Blaise Pascal – IFMA, Aubière, France

<sup>7</sup>Laboratoire de Mécanique et Génie Civil, UMR CNRS 5508, Université Montpellier 2, Montpellier, France

(\*)Email: [laurent.robert@mines-albi.fr](mailto:laurent.robert@mines-albi.fr)

## ABSTRACT

In order to characterise the ultimate error regime of Digital Image Correlation (DIC) algorithms, sets of virtual transformed images are often generated from a reference image by in-plane sub-pixel translations. This leads to the determination of the well-known S-shaped systematic error curves and their corresponding random error curves. It is reported in this collaborative work that the *a priori* choices used to numerically shift images (grey level interpolation, direct or reverse transformation between images) modify DIC results and may lead to biased conclusions in terms of DIC errors.

**Keywords:** Digital Image Correlation; Uncertainty quantification; Pattern matching; interpolation; Error assessment.

## INTRODUCTION

Digital Image Correlation (DIC) is an advanced experimental full-field measurement technique, which was first proposed in solid mechanics in the 80s' by Peters and Ranson (Peters, 1982). The basic principle of DIC is to match speckle patterns in grey level images of a sample in some reference and several deformed states, assuming convection of the grey level distribution during the transformation. The metrological assessment of such pattern matching procedures remains of high interest as there is still no normalisation or adapted procedures validated by the community of users. One way to characterise, at least partly, metrological performances of DIC algorithms is to experimentally generate displacement fields with precisely prescribed displacements or strains (Patterson, 2007). In practice, this approach is difficult (or even impossible) to implement because the actual value of the prescribed displacement field to be used as a reference for DIC measurements is often difficult to reach or control precisely; in addition it is often complex to separate the various error sources. Even for the simplest case of in-plane uniform sub-pixel image shifting, large difficulties arise with the classical translation experiment because of positioning and optical errors, stage imperfections, encoder errors, misalignments, motion drift, etc. The associated errors can alter the DIC error evaluation. An alternative way is to test DIC algorithms in

situations where displacement fields are numerically imposed between a reference and some transformed images. Within such a procedure, even if the reference image may be either a real image taken by a CCD camera or any other imaging tool or a synthetic one, the transformed image is always synthetically build from the reference one by some appropriate algorithm. Concerning DIC-displacement field accuracy assessment, the most common analysis is to consider uniform in-plane sub-pixel image translations, in order to construct the so-called S-shaped systematic error curve (Choi, 1997) and the associated random error curve, whose characteristics and amplitude depend on image properties and chosen DIC formulation and parameters. It has been shown in Bornert *et al.* (Bornert, 2009) that this error regime only corresponds to the “ultimate error regime” reached when the chosen subset shape function fits with a sufficient accuracy the actual displacement field. The purpose of the collaborative work presented in this paper is to emphasize that the *a priori* choices made to virtually translate images may have critical repercussions on the matching results as well as on the interpretation of the metrological performances of the investigated DIC algorithms.

## REFERENCE AND TRANSFORMED IMAGES

In the following, pairs of “undeformed”  $I_{\text{undef}}$  and “deformed”  $I_{\text{def}}$  images are considered. The correlation algorithms are applied to pairs of images corresponding respectively to an “initial”  $I_0$  and “final”  $I_1$  image. Note that this distinction is purely arbitrary since one can consider the direct ( $I_0 = I_{\text{undef}}$  and  $I_1 = I_{\text{def}}$ ) or the reverse ( $I_0 = I_{\text{def}}$  and  $I_1 = I_{\text{undef}}$ ) transformation. The metrological properties of the matching should neither depend on the chosen algorithm to transform images nor on the choice of reference image ( $I_{\text{def}}$  or  $I_{\text{undef}}$ ), but only on the image characteristics and the DIC algorithms under use (formulation and associated parameters). In the following, various methods to obtain sets of  $I_{\text{undef}}$  and  $I_{\text{def}}$  images are described and their influence on the characteristics of the systematic and random errors is discussed.

The question here is, first, to get a numerical undeformed image that best reflects an image obtained in real imaging conditions and, second, to shift it by specified displacements. To obtain such an image, the most natural way is undoubtedly to capture a real speckle pattern of a given specimen using the CCD camera (Roux, 2006) or the imaging device used for the measurements whose accuracy has to be assessed. The main advantage of this approach is that it allows to characterise the measurement errors using the most realistic images (exact speckle characteristics: size, grey level histograms and gradients, *etc.*; lighting conditions; ...). Nevertheless, this image may include some unwanted and unquantified features such as image noise (digitisation, read-out noise, black current noise, photon noise) or under or over sampling because of an imperfect CCD fill factor or optical imperfections, which will be hard to reproduce in the shifting procedure. Another solution is to numerically generate the image. Synthetic image generation indeed allows to prescribe most of the image characteristics (e.g. noise, speckle size, etc., see (Bornert, 2009) which can be quite useful for parametric studies of the performances of DIC algorithms). Naturally, the image should be generated in order to mimic as closely as possible the speckle patterns in a real experiment, for instance those obtained with classical spray painting. Efficient methods are based on the definition of a continuous luminance field named the texture function. The speckle image is generated by a photometric mapping and this texture function is digitized on a regular grid corresponding to each pixel of the image (Wattrisse, 2000; Zhou, 2001; Orteu, 2006).

The generation of the transformed images can generally be done by one of the three following methods:

- Interpolation of the undeformed image. It allows to create numerically shifted images on any type of image (real or computer-generated). It can be performed in the space domain by polynomial, spline or other interpolation schemes (Koljonen, 2008; Lava, 2009; Cofaru, 2010) or in the Fourier domain (Schreier, 2000; Roux, 2006). It is implicit that in this case the DIC error estimate also includes a contribution associated to the mismatch between the really advected image and the interpolated one.
- Oversampling of the undeformed image and generation of reference and deformed image by pixel averaging. This method can also be applied to real and synthetic images. For example, it has been applied by Doumalin *et al.* (Doumalin, 1999) for synthetic images of grids tracked by DIC, or more recently by Reu (Reu, 2011). In the latter reference images taken from an ultra-high definition CCD camera (4872×3248 pixels) are numerically binned by 10×10 pixels. This yields to final resolution images of 487×324 pixels shifted with respect to each other with a pitch of 0.1 pixel. Obviously only the translations of images are possible and a limited number of translation amplitudes is accessible.
- Transformation of the texture function. In the literature the speckle pattern is obtained by sampling an analytical function, that can be associated with the combination of individual Gaussian speckles (Wattrisse, 2000; Zhou, 2001) or with the Perlin noise function (Orteu, 2006). As the texture function is expressed in real space, any transformation of this texture function is easy to obtain and can be unbiased, assuming perfect convection of image intensity, in consistency with the fundamental assumption of DIC algorithms. Undeformed and transformed image are both obtained by a photometric mapping. This method does not, by nature, add bias in the deformed image, as its generation follows the same principles as for the reference one. The main drawback of this approach is to ensure that the texture function is representative of a real experimental speckle pattern and that the photometric mapping mimics the behaviour of a real optics and image sensor combination.

## IMAGE GENERATION AND METHODOLOGY

In this work, the  $I_{\text{undef}}$  image of size 1024×1024 pixels is a synthetic image obtained by photometric mapping and digitisation of a continuous speckle function in the real space (Orteu, 2006). Figure 1 shows several zooms of the  $I_{\text{undef}}$  image and its grey level histogram. Note that in this paper no random noise has been added to the images. The only image noise to be considered corresponds to the quantization errors, images being coded on 8 bits.

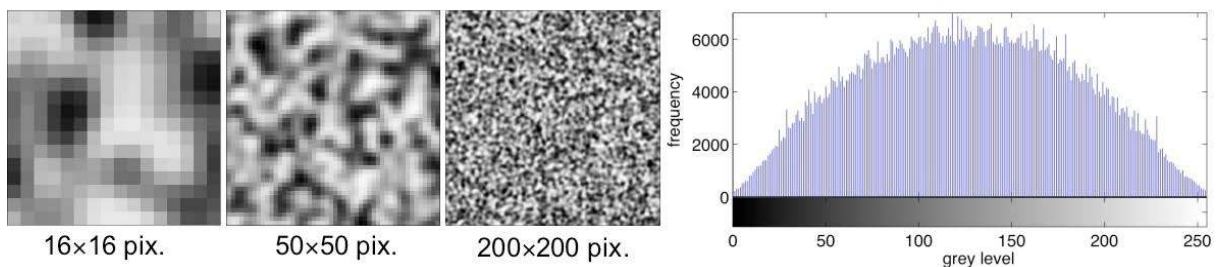


Fig.1. Left: sub-images of the synthetic images used in this work. Right: grey level histogram.

This choice of a synthetic reference image is governed by the fact that the  $I_{\text{def}}$  shifted images can be obtained in two different manners. On the one hand, they were obtained by interpolation of  $I_{\text{undef}}$  at non-integer locations using several interpolation schemes: polynomial interpolation (bilinear or bicubic), cubic spline interpolation, and interpolation based on Fourier transforms using the shift / modulation property. On the other hand, the translated images were obtained by translating the analytically known speckle function in the real space before mapping and digitization. The latter images are referred to as “TexGen images” in the following. In both cases, the imposed displacement  $u^{\text{imposed}}$  varies from 0 to 1 pixel with a step of 0.02 pixel. Note that the TexGen mapping and digitization procedure may be considered as a virtual imaging device, which is applied similarly to the reference and the rigorously shifted speckle function, so that results obtained with a couple of TexGen reference and deformed images can be considered as references with regard to results obtained with other image shifting strategies.

Images are analysed by a home-made DIC software that allows to select, if desired, the same image interpolation scheme than the one used to generate the shifted images  $I_{\text{def}}$  when using the image interpolation method to transform the images. This software is based on the minimisation of the classical Sum of Squared Difference (SSD) criterion with a zero-order subset shape function. It has been shown in Bornert *et al.* (Bornert, 2009) that subset shape function has little impact on simply shifted images. Subset size is set to 16×16 pixels.

The methodology to evaluate DIC errors is based on statistical analyses. The displacement error at the centre of a subset of coordinates  $(i,j)$  is defined by:

$$\Delta u_{ij} = u_{i,j}^{\text{measured}} - u_{i,j}^{\text{imposed}} \quad (1)$$

The standard deviation  $\sigma_u$  (random error) is calculated by:

$$\sigma_u = \sqrt{\frac{n \sum_{i,j} \Delta u_{ij}^2 - \left[ \sum_{i,j} \Delta u_{ij} \right]^2}{n(n-1)}} \quad (2)$$

where  $n$  is the number of calculated values while the arithmetic mean (systematic error, or bias) is obtained as:

$$\overline{\Delta u} = \frac{\sum_{i,j} \Delta u_{ij}}{n} \quad (3)$$

Displacements have been evaluated for all positions of a regular square grid in the initial image  $I_0$ , with a pitch of 16 pixels such that subsets at adjacent positions do not overlap ensuring the statistical independence of the corresponding errors. The output of this investigation is a set of two curves giving the evolution of the random (Equation (2)) and systematic (Equation (3)) errors as a function of the sub-pixel prescribed displacement along the horizontal direction of the images.

## RESULTS

We first focus on quantifications of DIC errors obtained when both  $I_{\text{def}}$  and (obviously)  $I_{\text{undef}}$  are TexGen images. Figure 2 presents the S-shaped curves giving the systematic error for various interpolation strategies of the DIC software, when considering both direct ( $I_0 = I_{\text{undef}}$

and  $I_1 = I_{\text{def}}$ , filled symbols) and reverse ( $I_0 = I_{\text{def}}$  and  $I_1 = I_{\text{undef}}$ , open symbols) transformation. Note that in the latter case the prescribed displacement  $u_{i,j}^{\text{imposed}}$  is simply the opposite of the one relative to the former.

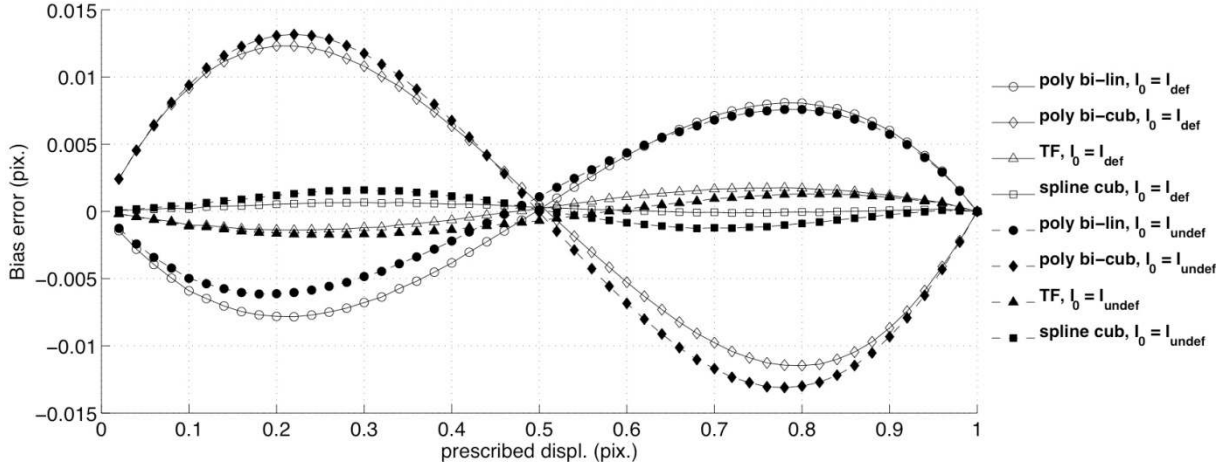


Fig.2 Systematic errors evaluated when considering pairs of TexGen images, for both direct ( $I_0 = I_{\text{undef}}$  and  $I_1 = I_{\text{def}}$ ) and reverse ( $I_0 = I_{\text{def}}$  and  $I_1 = I_{\text{undef}}$ ) transformations.

The following comments on these results can be made:

- first, all curves are central-symmetric with respect to the point (0.5, 0), as expected for isotropic texture. This is the consequence of the fact that a translation  $u$  of some image, with errors  $\Delta u$ , is equivalent to the translation  $-u$ , with errors  $-\Delta u$ , of the image deduced by central symmetry. Such a symmetric image is statistically equivalent to the initial image for such a texture. In addition, the translation  $-u$  is itself equivalent to the translation  $I-u$  regarding the 1-pixel periodicity of DIC errors. Averages of errors at  $u$  and  $I-u$  are thus opposite and standard deviations equal, as long as the set of measurement points considered for the statistical analysis is representative.
- the bias error is always present and its amplitude depends on the interpolation scheme used in the DIC software. As already reported (Schreier, 2000), spline interpolation diminishes this amplitude in comparison to classical polynomial interpolation: it is about  $2.4 \times 10^{-2}$  pixel for bi-cubic polynomial,  $1.5 \times 10^{-2}$  pixel for bi-linear polynomial and  $2 \times 10^{-3}$  pixel for bi-cubic spline interpolations. The sign of the systematic error depends on the interpolation used. The Fourier transform-based interpolation (noted TF in Fig. 2) also leads to very good results with a bias amplitude of about  $3 \times 10^{-3}$  pixel.
- bias curves relative to the direct ( $I_0 = I_{\text{undef}}$ ) or the reverse ( $I_0 = I_{\text{def}}$ ) transformations are very similar. The small differences for a given interpolation scheme can be attributed to statistical convergence effects.

Let us now focus on the random errors obtained in the same conditions. They are given in Figure 3, in which symbols have the same meaning as in Figure 2, and motivate the following comments:

- first, all random error curves are symmetric with respect to the vertical axis  $x = 0.5$ , for the same reasons as previously.

- random errors versus displacement present bell-shaped curves with one or two maxima depending on the DIC interpolation scheme. The amplitude of the maxima diminishes from about  $4 \times 10^{-3}$  pixel for bi-linear polynomial,  $2.4 \times 10^{-3}$  pixel for bi-cubic polynomial,  $1.6 \times 10^{-3}$  pixel for Fourier transform to  $1.4 \times 10^{-3}$  pixel for bi-cubic spline.
- as previously observed for the bias curves, random error curves do almost not depend on the choice of the direct ( $I_0 = I_{\text{undef}}$ ) or the reverse ( $I_0 = I_{\text{def}}$ ) transformation.

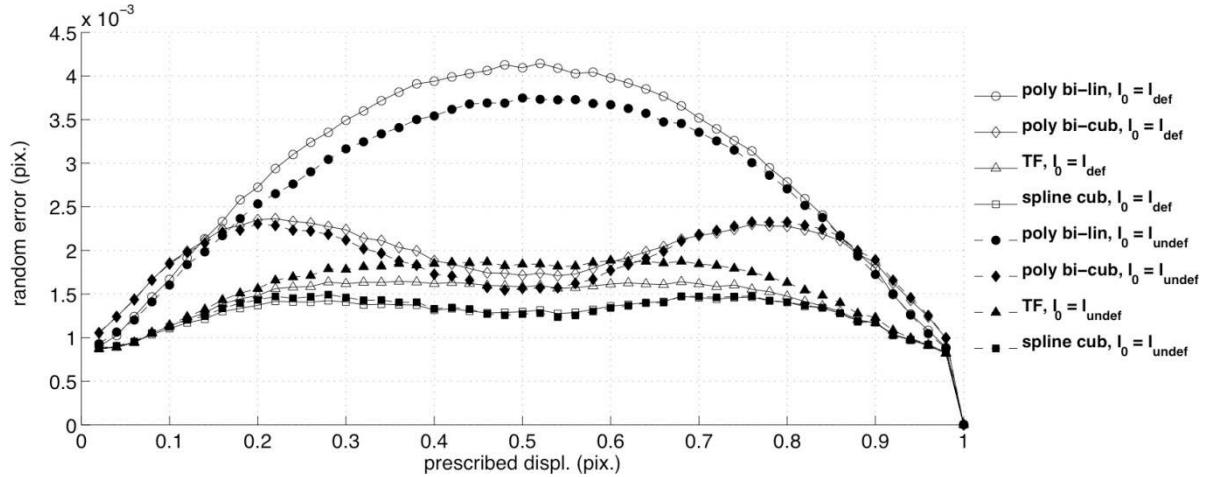


Fig.3 Random errors evaluated when considering pairs of TexGen images, for both direct ( $I_0 = I_{\text{undef}}$  and  $I_1 = I_{\text{def}}$ ) and reverse ( $I_0 = I_{\text{def}}$  and  $I_1 = I_{\text{undef}}$ ) transformation.

Consequently, both bias and random errors are mainly due to the TexGen image characteristics (grey level, speckle sizes and distributions, grey level gradients, *etc.*) and to the image processing algorithms implemented in the DIC software.

Let us now focus on the case when  $I_{\text{def}}$  shifted images are obtained by interpolation of  $I_{\text{undef}}$ . Here, the same interpolation scheme as the one applied for producing the deformed images is used in the DIC software. It is recalled that images have the same characteristics as previously, as the undeformed image ( $I_{\text{undef}}$ ) is the same TexGen image. Figure 4 (respectively Figure 5) presents the bias errors (respectively the random errors) *versus* prescribed displacements for various image interpolation strategies related to those of the DIC software, and considering both direct (filled symbols) and reverse (open symbols) transformations. Figures 4(a) and 5(a) present the full curves while Figures 4(b) and 5(b) highlight a zoom in the appropriate range.

Two main situations have to be analysed depending on whether the direct or the reverse transformation is considered.

When the direct transformation is considered, classical tendencies are recovered, but with different amplitudes depending on the interpolation scheme used to generate (and process) the images. For the bias error, amplitudes range from about  $8 \times 10^{-2}$  pixel for bi-linear polynomial interpolation,  $6 \times 10^{-3}$  pixel for bi-cubic polynomial interpolation,  $2 \times 10^{-3}$  pixel for Fourier transform, to  $1 \times 10^{-3}$  pixel for bi-cubic spline interpolation. Compared to those obtained from TexGen transformed images, these results show that bi-linear polynomial interpolation of the images to be analysed adds large systematic errors while surprisingly the bias amplitude for the bi-cubic interpolation of the images to be analysed ( $6 \times 10^{-3}$  pixel) is lower than the one

associated with the TexGen images ( $2.4 \times 10^2$  pixel). This phenomena have been notified recently by Reu (Reu, 2011).

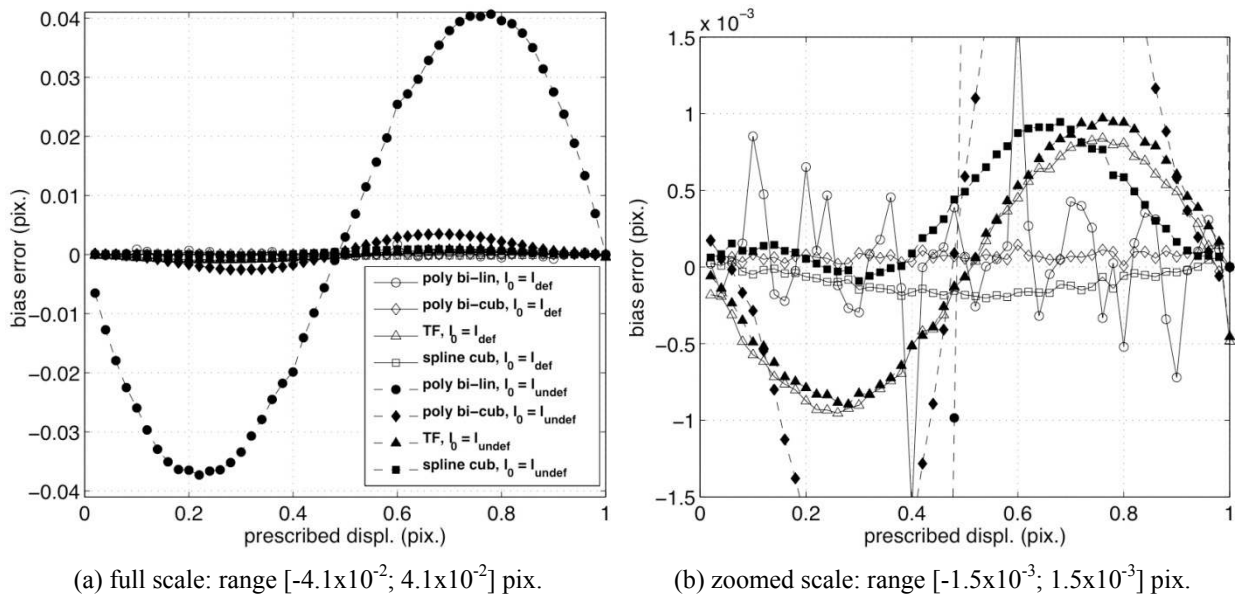


Fig.4 Systematic errors for both direct and reverse transformations, for various interpolation schemes used for both DIC analysis and image shifting.

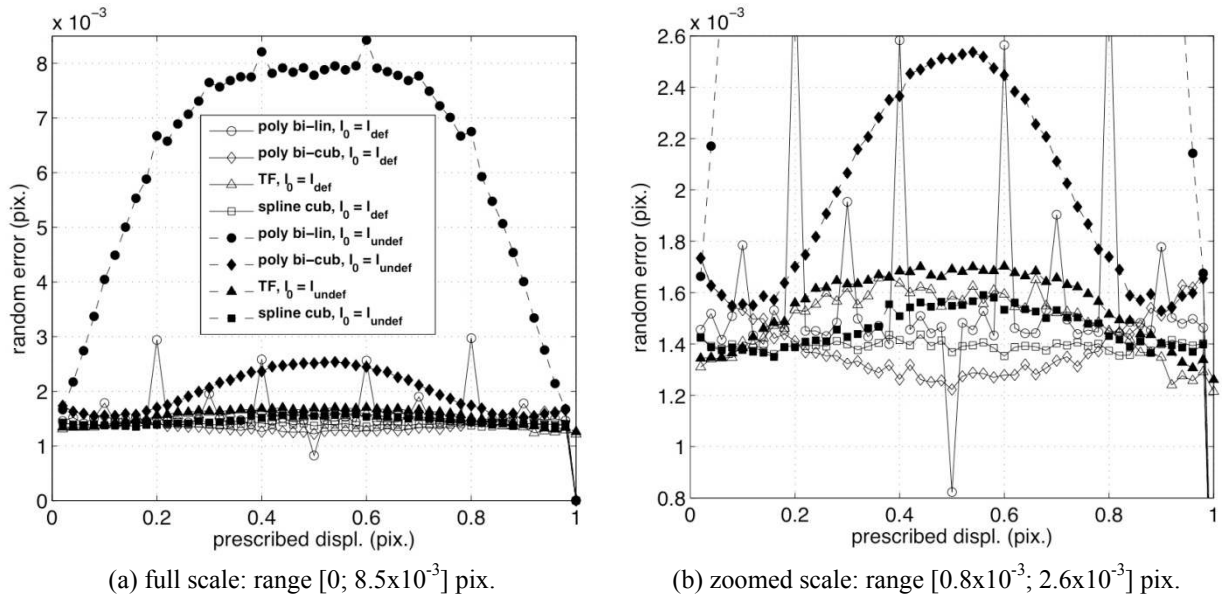


Fig.5 Random errors for both direct and reverse transformations, for various interpolations schemes used for both DIC analysis and image shifting.

If now we consider the reverse ( $I_0 = I_{def}$ ) transformation, it appears that an almost zero bias (except for the Fourier interpolation) is observed (see curves with open symbols in Figure 4(b)). Bi-linear interpolation shows however noisy values but within the  $\pm 5 \times 10^{-4}$  pixel range. No change is observed for the Fourier transform curves whatever the shifting method because the Fourier transform is a non-local process, which is not the same in DIC algorithms and image shifting: the whole image is used for the latter while in the former the FFT is only applied to a neighbourhood of the image subset the size of which is twice the subset size in



the present approach.

Considering the random error curves for the reverse ( $I_0 = I_{\text{def}}$ ) transformation (see Figure 5(b), open symbols), the main observation is that the random error decreases in general and becomes almost independent of the prescribed sub-pixel displacement, and a mean value of about  $1.4 \times 10^{-3}$  pixel is observed. As already seen for the bias curves, bi-linear interpolation also shows noisy values, and no change is observed for the Fourier transform curves whatever the transformation considered. Note finally that the value of about  $1.4 \times 10^{-3}$  pixel is the smallest value found for the random error with the TexGen images processed with the DIC bi-cubic spline interpolation (Figure 3) The same result is also found for the bi-cubic spline interpolation of the shifted image for the direct transformation, and not far for the reverse transformation.

From a general point of view, one may conclude that for the reverse transformation, the bias error should be almost non-existent because the transformation and then its inverse are computed exactly. The possible observed gap around zero may result from computation errors in the correlation criterion minimization or in the interpolation (*e.g.* Fourier transform). Concerning the random error, following Roux and Hild (Roux, 2006) or Wang *et al.* (Wang, 2009), the constant value of about  $1.4 \times 10^{-3}$  pixel can be linked to the standard deviation of the actual image noise  $\sigma_n$ , the average of the squared grey level gradient  $\overline{\nabla I^2}$  of the image and the subset size  $d$  considered in this work, according to:

$$\sigma_u^{th} \propto \frac{\sigma_n}{d\sqrt{\overline{\nabla I^2}}} \quad (1)$$

$\sqrt{\overline{\nabla I^2}}$  can be evaluated from the images to be 30 grey levels per pixel. With  $d = 16$  pixels, a value of  $\sigma_u^{th} = 1.4 \times 10^{-3}$  pixel is found for  $\sigma_n = 0.67$  grey levels, which gives a good order of magnitude of the image noise, only due to quantization in the present study.

## CONCLUSION

This work deals with the DIC “ultimate error regime” reached when the chosen subset shape function fits sufficiently well the actual displacement field. In this context, the evaluation of this ultimate error regime is generally done by real or synthetic images that are numerically shifted with sub-pixel rigid body motions. To that end, test images have been first transformed both by classical image interpolations and by transformation of an analytic texture function then mapped and finally digitized (TexGen images). Images have been processed using an appropriate DIC software. Results showed that when TexGen images are considered, bias and random errors are due to the image characteristics and the image processing by the DIC software, depending of its underlying interpolation scheme. When direct transformation is imposed ( $I_0 = I_{\text{undef}}$ ), classical tendencies are recovered but with different values depending on the interpolation scheme used to generate and processed images. If the reverse transformation is imposed ( $I_0 = I_{\text{def}}$ ), an almost zero bias (except for the Fourier interpolation) and a random error independent of the prescribed sub-pixel displacement is observed. These results illustrate the fact that such an evaluation of DIC error can be directly linked to the underlying assumptions taken to generate the synthetic shifted images, and thus may not be representative of the actual behaviour of the DIC software in some cases. It highlights the importance, for the assessment of sub-pixel accuracy of DIC packages, of using methods for creating images which can reproduce the physical process of creation of images.

## ACKNOWLEDGMENTS

The authors gratefully acknowledge the French CNRS (National Centre for Scientific Research) for supporting this research.

## REFERENCES

- Bornert M, Brémand F, Doumalin P, Dupré JC, Fazzini M, Grédiac M, Hild F, Mistou S, Molimard J, Orteu JJ, Robert L, Surrel Y, Vacher P, Wattrisse B. Assessment of Digital Image Correlation measurement errors: methodology and results, *Exp Mech*, 2009, 49, p. 353-370.
- Choi S, Shah S, Measurement of deformations on concrete subjected to compression using image correlation. *Exp Mech*, 1997, 37(3), p. 307-313.
- Cofaru C, Philips W, Van Paepegem W, Evaluation of digital image correlation techniques using realistic ground truth speckle images, *Meas Sci Technol*, 2010, 21, 055102.
- Doumalin P, Bornert M, Caldemaison D, Microextensometry by image correlation applied to micromechanical studies using the scanning electron microscopy. In: *Proceedings of the international conference on advanced technology in experimental mechanics*, 1999, Japan Soc Exp Eng, Ube City, Japan, p. 81-86.
- Koljonen JT, Alander JT, Deformation image generation for testing a strain measurement algorithm, *Opt Eng*, 2008, 47, 107202.
- Lava P, Cooreman S, Coppieters S, De Strycker M, Debruyne D, Assessment of measuring errors in DIC using deformation fields generated by plastic FEA, *Opt Las Eng*, 2009, 47, p. 747-753.
- Orteu JJ, Garcia D, Robert L, Bugarin F. A Speckle Texture Images Generator, *Speckle06*, Slangen, P and Cerruti, C, Eds, 2006, SPIE 6341.
- Patterson EA, Hack E, Brailly P, Burguete RL, Saleem Q, Siebert T, Tomlinson RA, Whelan MP, Calibration and evaluation of optical systems for full-field strain measurement, *Opt Las Eng*, 2007, 45(5), p. 550-564.
- Peters WH, Ranson WF, Digital Image Techniques In Experimental Stress Analysis, *Opt Eng* 1982, 21, p. 427-432.
- Reu PL, Experimental and Numerical Methods for Exact Subpixel Shifting, *Exp Mech*, 2011, 51(4), p. 443-452.
- Roux S, Hild F, Stress intensity factor measurements from digital image correlation: post-processing and integrated approaches, *Int J Fract*, 2006, 140, p. 141-157.
- Schreier H, Braasch J, Sutton M, Systematic errors in digital image correlation caused by intensity interpolation. *Opt Eng*, 2000, 39(11), p. 2915-2921.
- Wang YQ, Sutton MA, Bruck HA, Schreier HW, Quantitative Error Assessment in Pattern Matching: Effects of Intensity Pattern Noise, Interpolation, Strain and Image Contrast on Motion Measurements, *Strain*, 2009, 45, p. 160-178.
- Wattrisse B, Chrysochoos A, Muracciole JM, Némot-Gaillard M., Analysis of strain localization during tensile tests by digital image correlation, *Exp Mech*, 2000, 41, p. 29-39.
- Zhou P, Goodson KE, Subpixel displacement and deformation gradient measurement using digital image/speckle correlation (DISC), *Opt Eng*, 2001, 40, p. 1613-1620.